This article has been accepted for publication in a future issue of this journal, but has not been fully edited. Content may change prior to final publication. Citation information: DOI 10.1109/JPHOT.2016.2528126, IEEE Photonics Journal

Pre-Amplified Demodulation of 56 Gbs WDM DPSK Signals by an AWG-based InP-PIC

Philippe Velha, Nicola Andriolli, and Giampiero Contestabile

Scuola Superiore Sant'Anna, Via G. Moruzzi 1, 56124, Pisa, Italy
**Corresponding author: contesta@sssup.it*

Received Month X, XXXX

A compact pre-amplified receiver for WDM-DPSK signals based on Gaussian filtering is proposed, simulated, and a first implementation including an SOA and an ad-hoc arrayed waveguide grating (AWG) is demonstrated by monolithical integration in an InP platform. The demodulation of 56 Gb/s channels on the eight, 100-GHz-spaced, AWG outputs is experimentally reported and simulation results show the feasibility of multiwavelength operation obtaining simultaneous demultiplexing and demodulation of all the channels. The resilience to chromatic dispersion for the Gaussian filter demodulation is also shown by simulations.

1. INTRODUCTION

Differential phase shift keying (DPSK) is a pure phase binary modulation format which shows enhanced resilience to nonlinear effects and ~ 3-dB enhanced sensitivity in back to back in respect to intensity modulated direct detection (IM-DD) systems if conventional demodulation by a 1-bit delay interferometer is performed together with the use of balanced detection [1]. This implies that, in case of wavelength division multiplexed (WDM) systems, a full receiver requires the use of a delay interferometer and a balanced detector for each of the channels (see Fig. 1a), so that a number of receiving boards with related power consumption and footprint are necessary in order to realize a practical WDM-DPSK receiver. This bulky arrangement can be undesirable in various network scenarios in which high density port count is a critical aspect as, for example, large bandwidth metro and access networks. An alternative demodulation scheme, not requiring interferometers, can be realized through ad-hoc filtering with Gaussian filters whose bandwidth is 2/3 of the bitrate [2, 3]. So doing, even if the ~ 3-dB sensitivity advantage in back to back is lost, the transmitted channels are made more resilient to fiber chromatic dispersion [2, 3]. Moreover, this scheme can be implemented in a very compact way with the use of photonic integrated circuits (PICs), as in the example sketched in Fig. 1b. A single properly designed AWG can simultaneously perform WDM demultiplexing and DPSK demodulation in a single shot for all the channels, and the demultiplexed channels can be simply received by a conventional photodetector. If available in the integration platform, a common pre-amplification stage can be included and integrated at the input of the WDM receiver in order to boost up the received input power levels accounting also for the device coupling and insertion losses. Using this scheme, the integration of a full WDM-DPSK receiver on single transmission board is possible in principle as the receiver can be made similar to the one for IM-DD signals, i.e., made by an AWG and *n* photodiodes. In this paper a practical implementation of this concept by using an InP integration platform is reported including simulation and experimental results obtained with a PIC performing the demodulation of 8 100GHz-spaced channels at 56 Gb/s. However, as high speed integrated photodiodes were not available in the fabrication process, in this first demonstration of the circuit external photodetectors have been used instead of monolithically integrated ones. Also, the InP PIC is polarization dependent, so the fabricated circuit can detect a single polarization signal only. Polarization diversity or a polarization independent AWG are required in order to obtain a polarization independent receiver. In particular, this paper summarizes the results previously shown in [4, 5] and, thanks to the additional simulative results, shows the potentiality of the scheme in terms of WDM operation and resilience to crosstalk and wavelength instability.

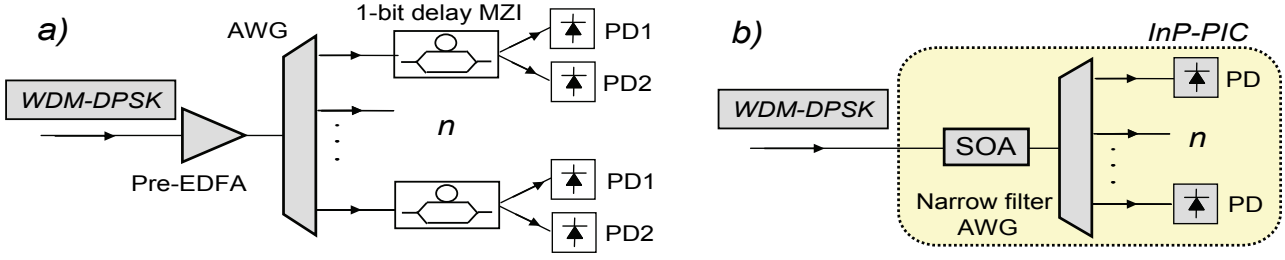

Figure 1. a) Scheme of a conventional WDM-DPSK receiver. b) Scheme of the integrated pre-amplified receiver for WDM-DPSK signals based on narrow filtering.

This article has been accepted for publication in a future issue of this journal, but has not been fully edited. Content may change prior to final publication. Citation information: DOI 10.1109/JPHOT.2016.2528126, IEEE Photonics Journal

2. INP-PIC FABRICATION AND EXPERIMENTAL RESULTS

The PIC, which reproduces in practice the scheme of Fig. 1b, consists of an input angled waveguide, a 1-mm-long SOA plus an ad-hoc designed 1×8 AWG. 8 output angled waveguides are then realized in order to couple out the demultiplexed and demodulated DPSK signals, as on-chip photodetectors were not available in the fabrication platform. The designed layout and the realized device are reported in Fig. 2. The total PIC footprint is 3 mm^2. The AWG has been designed with a Gaussian shape, a central frequency at 1545 nm, a free-spectral range of 6.4 nm, a channel spacing of 0.8 nm. The PIC was fabricated using the JePPIX technology platform [6]. This generic fabrication platform offers a set of standard photonic building blocks such as shallow and deeply etched passive waveguides, SOAs, and phase shifters. Custom made circuits can be designed using these building blocks. Different PICs can be combined on a multi-project wafer (MPW) run and fabricated simultaneously at the COBRA research institute. All the details of the fabrication process can be found in ref. [6]. Thanks to a deep-shallow double etching technique the AWG is designed such that losses and reflections are minimized.

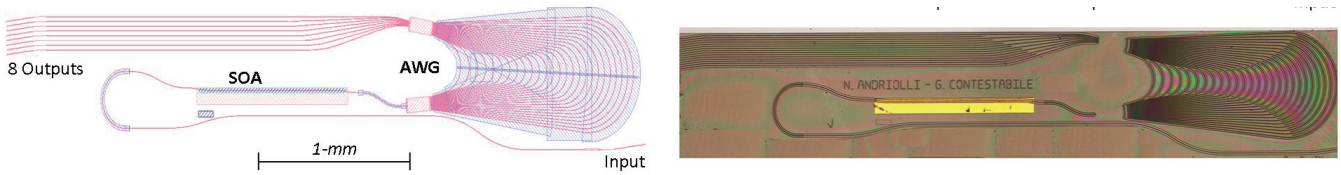

Figure 2. Mask design (left part) and a microscope picture (right part) of the fabricated InP PIC. Footprint: ~ 3 (4.3x0.7) mm^2.

Characterization of the 1-mm-long SOA preamplifier made on a sample structure at 200 mA bias current is reported in Fig. 3, left and central part, all values are given on-chip. The small signal gain as a function of the wavelength is reported in the left part of Fig. 3. The gain and power values are obtained with an estimated input/output coupling loss of 6 dB (giving 12 dB total PIC coupling loss, as spot size converters for optimizing the fiber coupling were not available in the fabrication process). Maximum gain is 14.8 dB at the 1532 nm peak. The input/output power characteristic is reported in the central part of Fig. 3 for λ=1548 nm. The resulting 3 dB input saturation power is -1 dBm.

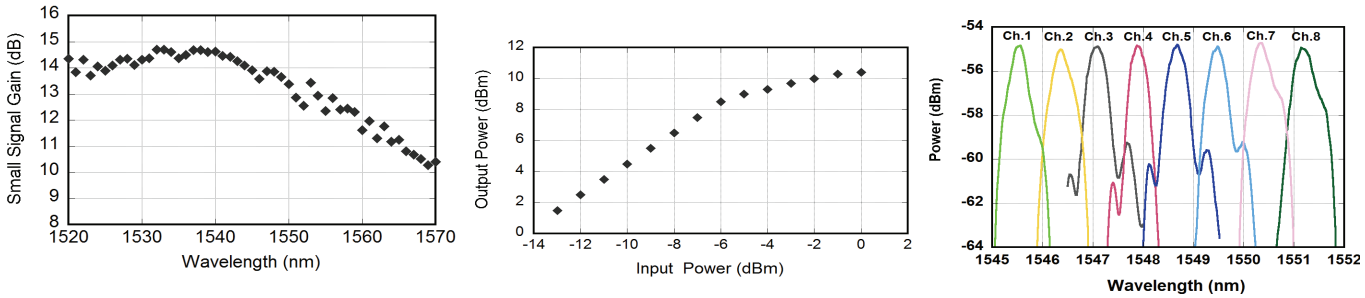

Figure 3. SOA preamplifier small signal gain (left part) and input/output power characteristic (central part). All the values are on-chip values extrapolated assuming 6 dB coupling loss for facet. On the right, AWG output spectra, channel spacing is 0.8 nm (100 GHz).

The AWG pass-band spectra recorded at the 8 different output waveguides exploiting the amplified spontaneous emission (ASE) from the integrated SOA are reported in the right part of Fig. 3 (channels are normalized to the same amplitude). The channel separation is 0.8 nm (100 GHz) ranging from 1545.6 to 1551.2 nm in agreement with the design and the 3-dB bandwidth was measured to be (37±2) GHz, which is appropriate for the demodulation of 56 Gb/s channels [2]. Insertion losses for the AWG channels were in the range (8±3) dB. Unfortunately, the bandpass shape of the fabricated AWG is not uniform for all the channels and also undesired spectral side-lobes are clearly present in the spectra: the reason for this un-ideal shape is to be attributed to the polarization conversion effect occurring in the curved arrayed waveguides, as described and discussed in detail in [7], where similarly designed AWGs have been tested. In the same paper, improved design rules are also proposed for improving the AWG transfer function. Nonetheless, even if the large crosstalk resulting from the spectral response of Fig. 3 strongly limits WDM demultiplexing operation, as reported in the following, proper DPSK demodulation has been possible for all the 8 single channels of the AWG.

The experimental setup for the PIC test is reported in Fig. 4. A tunable DPSK transmitter is realized using a tunable laser and a 40 GHz Mach-Zehnder modulator (MZM) biased at the maximum of the transfer function and driven by 2^{23}-1-long pseudo random bit sequences at 56 Gb/s generated by a pattern generator. The signal is amplified by an EDFA and filtered by a 1-nm-wide band-pass filter. The input optical power to the chip is controlled by a variable optical attenuator. Input polarization is adjusted with an external fiber polarization controller. Tapered fibers with a focused spot size of around 2.5 μm are used for input/output coupling to the chip and PIC temperature is

This article has been accepted for publication in a future issue of this journal, but has not been fully edited. Content may change prior to final publication. Citation information: DOI 10.1109/JPHOT.2016.2528126, IEEE Photonics Journal

controlled and fixed at 25°C thanks to a Peltier cooler. The output signals are individually collected by the 8 different output waveguides and then amplified by an EDFA, filtered by a 1-nm-wide band-pass filter and sent to both a sampling oscilloscope with a 53 GHz optical head and a 35 GHz amplified photoreceiver for BER measurements. The output optical amplification stage is used in order to guarantee enough power for monitoring the input/output optical alignment but is not required for the PIC operation. The signal collected by the photoreceiver is sent to the error detector which is synchronized by an electrical clock signal at half-rate (28 GHz) sent from the pattern generator.

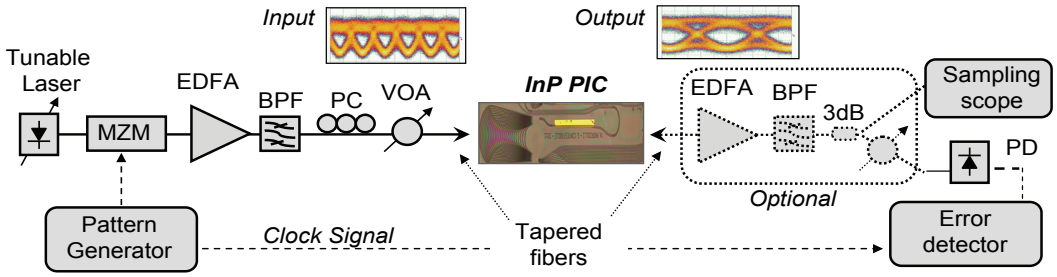

Figure 4. Experimental set-up. MZM= Mach-Zehnder Modulator; PC= Polarization Controller; EDFA= Erbium Doped Fiber Amplifier; BPF= Optical Band-Pass Filter, VOA= Variable Optical Attenuator; PD= Photodetector. In the inset, the input and output eye diagrams for a 56 Gb/s channel.

The DPSK demodulation obtained by narrow filtering of channel 3 at 1547 nm is shown in Fig. 5. On the left part, the 56 Gb/s DPSK signal input and output spectra from the PIC and the corresponding eye diagrams are reported as recorded by an optical spectrum analyzer and by the 53 GHz optical head of the oscilloscope. The input signal shows the typical symbol intensity transitions generated by a DPSK transmitter based on a MZM. The demodulated and wide open 56 Gb/s output eye diagram is obtained because of phase to intensity conversion by narrow filtering, i.e., same consecutive symbols (data persistence), which are spectrally close to the carrier, pass through the filter unaffected. Data transitions, which are aside in the spectrum, are cancelled. BER measurements results for all the 8 output channels are performed by tuning the 56 Gb/s transmitter and are summarized in the same figure (central part). All the measurements are performed by changing the input power to the PIC while keeping a fixed power of -3 dBm on the 35 GHz photoreceiver (using the EDFA at the output). As it can be seen, all the channels reach a BER better than 10^{-9} without any floor tendency and the sensitivity at 10^{-9} is in the range 4 - 9 dBm depending mainly on the different filtering shape and AWG channel loss. The eye diagrams for channel 3 reported in Fig. 5 correspond to the worst performing received channel.

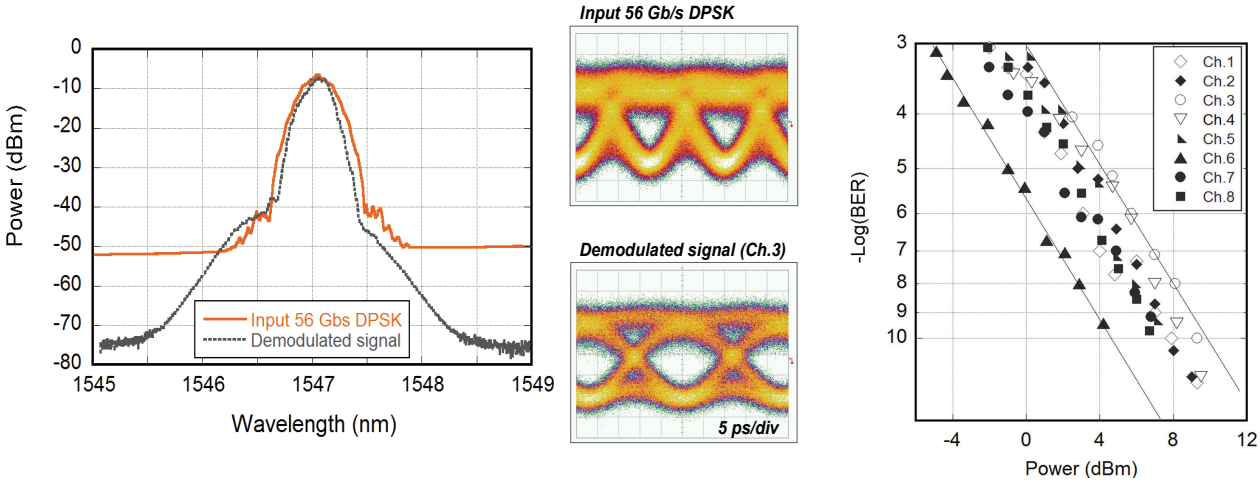

Figure 5. (Left part) 56 Gb/s input and output spectra to/from the integrated demodulator. Correspondent input and demodulated eye diagrams for are reported. (Right part) BER measurement results for the 8 AWG channels.

The resulting sensitivity values are strongly affected by a number of non-ideal factors, namely, the PIC coupling input/output losses, the limited bandwidth of the photoreceiver available for the measurement (35 GHz), and the limited on-chip gain of the integrated SOA. Clearly, significant improvements are possible in different ways: by the use of on-chip spot size converters [8] (thus reducing the coupling insertion loss from 6 to 2-3 dB); by the monolithic integration of the photoreceivers on the chip, so removing completely the output coupling loss; and by using an on-chip SOA with a larger gain as, for example, the one reported in [9] fabricated using an alternative technology platform. All these considered, a 15 dB improvement of the sensitivity can be reasonably envisioned considering a 6 dB reduced insertion loss and an SOA with around 25 dB on-chip gain. In the case of integrated fast photodetectors the sensitivity will strongly depend on the characteristics of those and the available transimpedance amplifier.

As mentioned before, WDM operation was not possible because of the non-ideal spectral shape of the fabricated AWG, i.e. the resulting channel isolation was not enough to guarantee proper WDM demodulation and demultiplexing. It should be considered, however, that InP AWGs with the requested channel isolation can nowadays be fabricated using alternative technology platforms [10]. In the following sections, simulation results are reported in order to study the feasibility of WDM operation and the impact of the related crosstalk on the receiver performance.

3. WDM-DPSK DEMODULATION: SIMULATION RESULTS

Simulations of the WDM-DPSK receiver made by Gaussian filtering are performed using the Interconnect software of the Lumerical Inc. simulation suite. In order to focus the analysis on the distortions generated by the DPSK-WDM demodulation and demultiplexing, and considering that SOAs operated in the proper linear regime are not a source of significant noise and nonlinear effects, especially for WDM-DPSK signals [11,12], we did not consider the SOA in the simulations. An 8-channel WDM DPSK transmitter is designed using 8 100GHz spaced lasers and MZIs driven at the maximum of the transfer function with decorrelated 2^{11} long PRBS sequences (for the sake of computational time). The signals are therefore sent in a multiwavelength Gaussian filter having a resulting spectral response like the one reported in Fig. 6 (left part, black line). The multiwalength filter is made by 8 Gaussian filters having central frequencies corresponding to the transmitter lasers (from 1545.6 to 1551.2 nm or 193.64 THz to 194.34 THz) and a 3-dB bandwidth of 37.3 GHz. The resulting channel isolation at 100 GHz is 40 dB. The 8 demodulated and demultiplexed channels recorded on the output ports are reported in the same figure with different colors. Example of the resulting eye diagrams are also shown for the more external wavelengths and for channel 4, which is (together with its symmetric channel 5) the most affected by crosstalk from adjacent channels. As it can be seen, demodulation and demultiplexing can be properly obtained, even if with a different quality, depending on the wavelength allocation of the channels. Clearly the external channels show a reduced crosstalk in respect to the inner channels (ASE noise is not included in the simulation in order to isolate the channel crosstalk effect). A Q-factor of 11.5 is simulated for channel 1 compared to 8.4 for channel 4. In the right part of Fig. 6, the eye diagram for channel 4 is also compared with the case single channel demodulation.

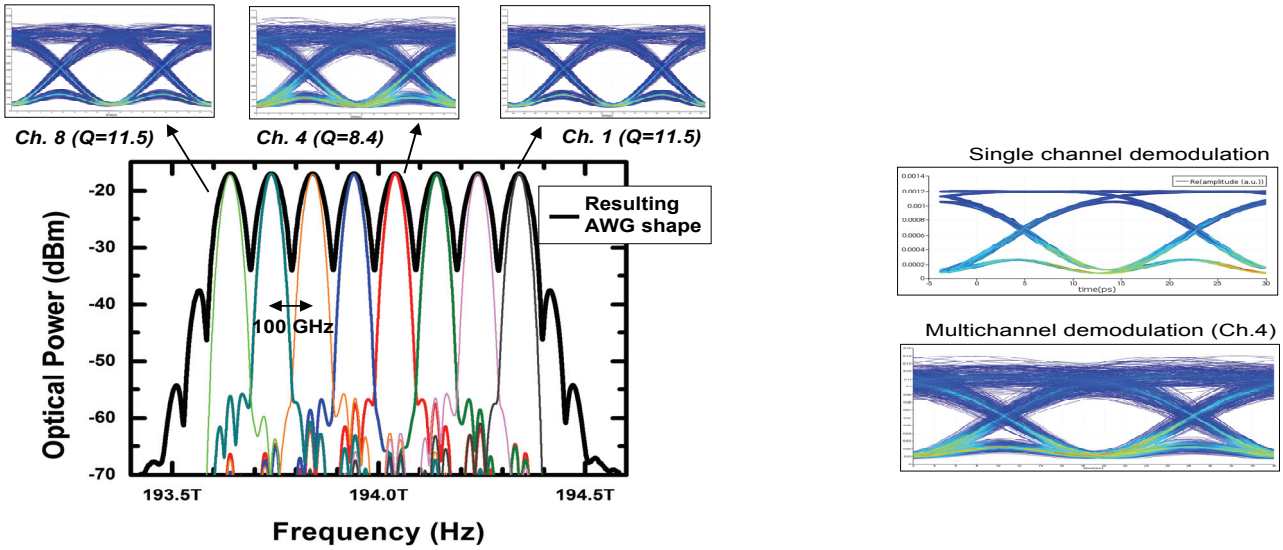

Figure 6. (Left part) Spectral shape of the multiwavelength Gaussian filter with demultiplexed and demodulated channels as recorded on the output waveguides. In the inset, example of eye diagrams for channels 1, 4 and 8. (Right part) Effect of crosstalk on the eye diagram, comparison of single channel and multichannel demodulation.

BER curves are also extrapolated from the simulated eye diagrams through the Q-factor analysis*. The results comparing the BER curves for the single-channel and 8-channel Gaussian filtering and the single-channel conventional MZI demodulation with balanced detection are reported in Fig. 7a. For the 8-channel case, channel 1 and channel 4 are considered as test channels. As it can be seen, single-channel Gaussian demodulation loses the 2.6 dB sensitivity advantage in respect to conventional balanced detection and multichannel operation suffers from additional penalty and a different trend depending on the wavelength allocation. External signals (e.g., channel 1) have an additional 3 dB power penalty and floor tendency at 10^{-12} BER. Central signals like channel 4 suffer from a floor at 10^{-9} BER. Unfortunately, due to the BER extrapolation procedure the reliability of the results obtained at such

* BER extrapolation from the Q-factor is a precise approximation only in case of signals being Gaussian noise limited. Crosstalk noise does not typically follow a Gaussian distribution, so in this case this extrapolation is less accurate. Nevertheless, this simple BER estimation is a useful tool to provide an indication on the effect of the crosstalk in case of multiwavelength operation.

This article has been accepted for publication in a future issue of this journal, but has not been fully edited. Content may change prior to final publication. Citation information: DOI 10.1109/JPHOT.2016.2528126, IEEE Photonics Journal

a low error rate cannot be guaranteed. Nevertheless, proper operation at the conventional FEC limit value (BER equal to $2 \cdot 10^{-3}$) with 1.5÷2 dB additional penalty in respect to single wavelength operation is granted by the simulations even for the worst performing channels.

Additional simulations have been performed in order to study the resilience of this scheme to filter detuning from the nominal channel center. The results are reported in Fig. 7b where the BER as a function of the filter detuning is reported for the two cases, single-channel and 8-channel Gaussian filter based demodulation. Clearly, single-channel demodulation is more robust and tolerates an ±18 GHz detuning without significant BER degradation. 8-channel operation (channel 4 is used as test channel also in this case) is less robust because of crosstalk from adjacent channels so that a smaller detuning of ±10 GHz can be tolerated without significant BER reduction.

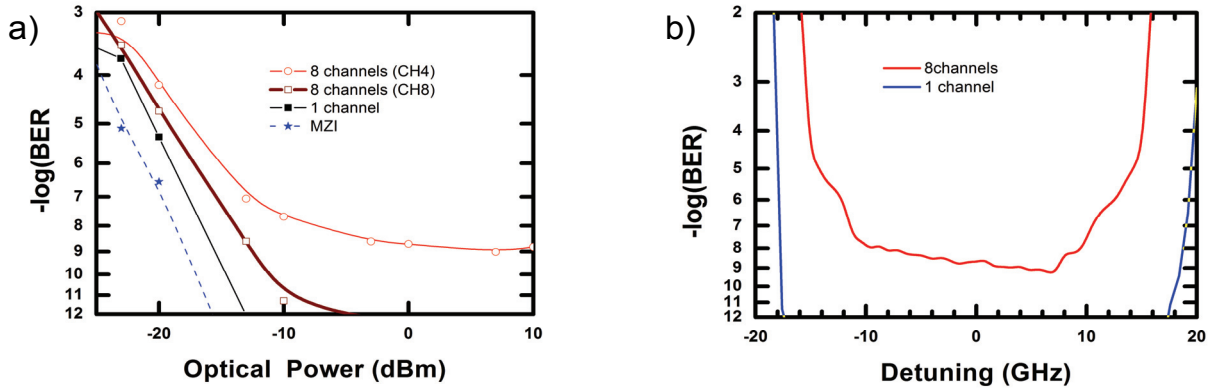

Figure 7. a) BER comparison for conventional DPSK demodulation by MZI and Gaussian filtering single and multichannel. b) Effect of filter detuning on signal BER.

When the chromatic dispersion tolerance is taken into account as well, we obtain the results summarized in Fig. 8 for the different modulation formats after fiber propagation. The BER for single-channel transmission in case of DPSK Gaussian filter demodulation, DPSK MZI-balanced demodulation and conventional NRZ single-ended receiver are reported as a function of transmission length in standard single-mode fiber with a chromatic dispersion index of 17 ps/(nm·km) at 1550 nm. As it can be seen and expected from theoretical analysis [2] and also experimental evidence at different bit-rates and using alternative filtering schemes [3, 13], the sensitivity advantage of the MZI demodulation in back to back is suddenly lost against chromatic dispersion in respect to NRZ and Gaussian demodulation. After around 2500 m, Gaussian filtered DPSK starts outperforming the other modulation formats being the only with a BER under the FEC limit for transmissions up to 10 km. The advantage in eye opening after propagation can also be seen looking at the evolution of the eye diagrams in propagation as reported in the right part of Fig. 8. After 1 km the NRZ signal has the best eye opening, but after 5 km the Gaussian filtered DPSK becomes the most resilient modulation format to chromatic dispersion.

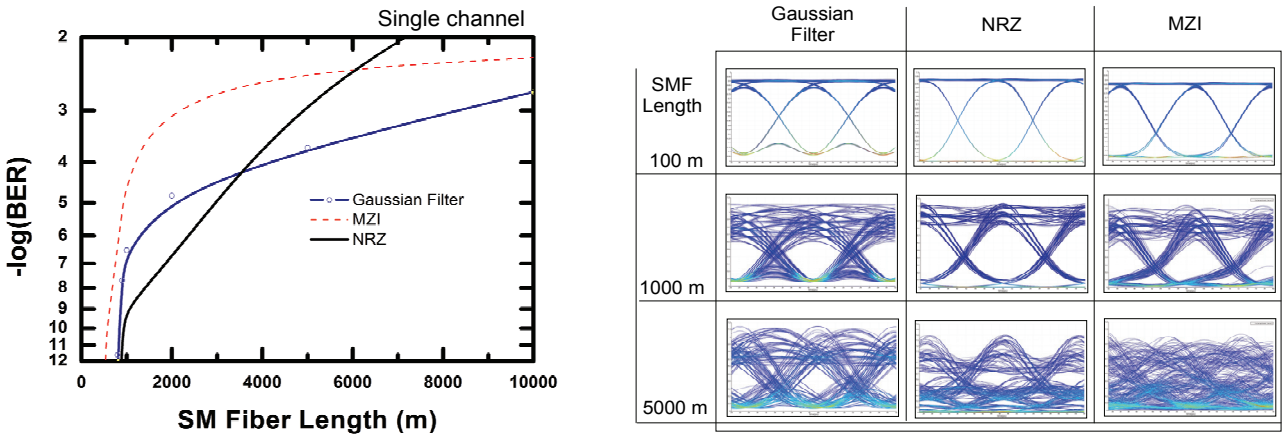

Figure 8. (Left part) Single channel BER comparison vs. fiber propagation (only dispersion) for conventional DPSK demodulation by MZI, Gaussian filtering and conventional NRZ. (Right part) Comparison of the eye diagrams.

A similar trend can be found in the WDM case. The BER results are reported for this case in Fig. 9 (8 channels as in Fig. 6, channel 4 used as test). The crosstalk limits the overall sensitivity performance but again the Gaussian filtered DPSK format performs better than the others, almost 10 km transmission at FEC limit can be obtained also in the WDM case.

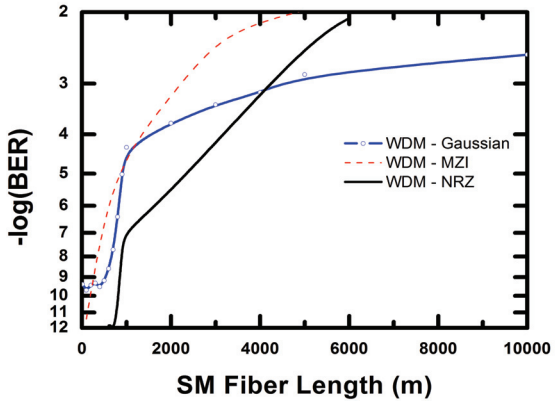

Figure 9. WDM case BER comparison (for channel 4) vs. fiber propagation (only dispersion) for conventional DPSK demodulation by MZI, Gaussian filtering and conventional NRZ.

4. CONCLUSIONS

Results about an InP integrated receiver for WDM-DPSK demultiplexing and demodulation based on an AWG Gaussian filter with eight, 100-GHz-spaced, channels and including an SOA as preamplifier have been reported. The PIC is proposed for the simultaneous demultiplexing and demodulation of 8 × 56 Gb/s WDM-DPSK signals. In this paper, we reported the experimental characterization of the device for all the 8 channels using a single tunable transmitter. Indeed, WDM operation was not possible because of the un-ideal spectral shape of the fabricated AWG, i.e., the resulting channel isolation was not enough to guarantee proper WDM demodulation and demultiplexing. In order to assess the feasibility of WDM operation we performed additional simulations showing that, despite a degradation of the signal quality because of crosstalk from adjacent channels, multiwalength operation is possible, in principle, using multiwavelength Gaussian filters with improved features. The resilience of the Gaussian filtered DPSK to chromatic dispersion is also reported by simulations showing that WDM 10 km transmission at 56 Gb/s is possible, in principle, with a BER under the FEC limit.

Finally, it is worth noting that a PIC receiver with a larger channel count is possible simply using a modified AWG with additional output channels and a significant improvement in performance and compactness of the circuit is possible by the monolithic integration of photoreceivers on the chip, removing the output coupling losses and allowing a very compact version of the integrated WDM receiver.

ACKNOWLEDGMENTS

The authors would like to acknowledge Prof. X. Leijtens and Dr. J. Bolk of Technical University of Eindhoven for the support in the PIC design and fabrication, and Mr. G. Dell'Orto of Anritsu Italia for the lending of the 56 Gb/s BERT. This work was partially supported by the Scuola Superiore Sant'Anna through the ESPION and ILAMPO projects.

REFERENCES

[1] A.H. Gnauck and P.J. Winzer, "Optical phase-shift-keyed transmission," *J. Lightwave Technol.*, Vol. 23, pp. 115-130 (2005)

[2] E. Forestieri and G. Prati, "Narrow filtered DPSK implements order-1 CAPS optical line coding," *IEEE Photon. Technol. Lett.*, vol. 16, pp. 662-664 (2004)

[3] A. D'Errico, R. Proietti, L. Giorgi, G. Contestabile, E. Ciaramella, "WDM-DPSK detection by means of frequency-periodic Gaussian filtering," *Electron. Lett.*, vol. 42, pp.112-114 (2006)

[4] G. Contestabile, P. Velha, and N. Andriolli, "An integrated and pre-amplified demodulator for 56 Gb/s WDM-DPSK signals," *International Conference on Photonics in Switching (PS)*, 2015, pp. 64-66 (2015)

[5] G. Contestabile, P. Velha, and N. Andriolli, "High-Speed InP-Integrated Pre-Amplified Demodulator for WDM-DPSK Signals," *IEEE Photon. Technol. Lett.*, vol. 27, pp. 2547-2550 (2015)

[6] X. Leijtens, "JePPIX: the platform for Indium Phosphide-based photonics," *IET Optoelectron.*, vol. 5, pp. 202-206 (2011)

[7] E. Kleijn, P.J. Williams, N.D. Whitbread, M.J. Wale, M.K. Smit, X.J.M. Leijtens, "Sidelobes in the response of arrayed waveguide gratings caused by polarization rotation," *Opt. Express*, vol. 20, pp. 22660-22668 (2012)

[8] F. Wu, V. I. Tolstikhin, A. S. Densmore, S. Grabtchak, "Two-step lateral taper spot-size converter for efficient fiber coupling to InP-based photonic integrated circuits," *Proceedings of the SPIE*, Volume 5577, pp. 213-220 (2004)

[9] N. Andriolli, S. Faralli, F. Bontempi, and G. Contestabile, "A wavelength-preserving photonic integrated regenerator for NRZ and RZ signals," *Opt. Express*, vol. 21, pp. 20649-20655 (2013)

[10] J.H. Baek et al. "10-GHz and 20-GHz Channel Spacing High-Resolution AWGs on InP," *IEEE Photon. Technol. Lett.*, vol. 21, pp. 298-300 (2009)

[11] R. Proietti, A. D'Errico, L. Giorgi, N. Calabretta, G. Contestabile, and E. Ciaramella, "16×10 Gb/s DPSK Transmission Over 140-km SSMF by Using Two Common SOAs," *IEEE Photon. Technol. Lett.*, vol. 18, pp. 1675-1677 (2006)

[12] A. D'Errico, G. Contestabile, S. Betti, V. Carrozzo, F. Curti, M. Guglielmucci, and E. Ciaramella, "Field-trial of SOA-based WDM-DPSK 8x10 Gbit/s system over 300km with conventional amplification span," *Electr. Lett.*, vol.43, pp. 404-405 (2007)

[13] G. Contestabile, R. Proietti, N. Calabretta, M. Presi, A. D'Errico, E. Ciaramella, "Simultaneous Demodulation and Clock-Recovery of 40-Gb/s NRZ-DPSK Signals Using a Multiwavelength Gaussian Filter," IEEE Photon. Technol. Lett., vol. 20, pp. 791-793 (2008)